OPTIMIZATION OF THE CIRCULAR MANHOLE COVER MADE OF DUCTILE CAST IRON USING FINITE ELEMENT METHOD

Assist. Prof. Lovrenić-Jugović M. PhD.[1], Assoc. Prof. Glavaš Z. PhD.[1], Assoc. Prof. Štrkalj A. PhD.[1], Assoc. Prof. Slokar Lj. PhD.[1], B.Sc. Radišić F.
University of Zagreb, Faculty of Metallurgy, Croatia [1]

mlovrenic@simet.hr

Abstract: *In this paper, in order to dimension the position and the number of vertical reinforcement, several numerical linear static simulations of bending circular manhole cover of ductile cast iron (grade EN-GJS-500-7) with 600 mm diameter are performed. The analysis of displacement and stress using the finite element method in the software package Autodesk Simulation Mechanical were conducted. Verification of numerical results for the solution of thin circular plate was performed with analytical bending solutions. After checking the numerical procedure on the thin circular plate, two circular vertical reinforcements were added on the underside: internal and external. Numerical simulations investigated the influence of the inner circular reinforcement position on the strength of the circular manhole cover, while equivalent stresses followed by energy theory of strength (von Mises) were monitored. Since maximal equivalent stresses remain on the plate by varying the position of the inner circular reinforcement, simulations with added radial reinforcements are performed. Finally, by optimizing the number of radial reinforcements, the optimum plate design is chosen.*

Keywords: CIRCULAR MANHOLE COVER, VERTICAL REINFORCEMENTS, LINEAR ANALYSIS, FINITE ELEMENT METHOD, DUCTILE CAST IRON

1. Introduction

Modern civilization cannot be imagined without a system of drainage of waste and precipitation water. Manhole covers are essential functional and safety parts of the system. They must allow access to the system, i.e. to be mobile, but also must have the required strength.

Manhole covers are circular or square plates, which are generally located on pavements or roads. They must be very strong and durable to be able to withstand the load and impact of pedestrians and/or vehicles' constant weight upon them. They are generally made out of cast iron. The circular shape for the manhole cover allows easier transporting by rolling as well as manufacturing, installing and maintaining [1,2].

Installation place according to classes of manhole cover are presents in [3]. Covers class D 400 (Fig. 1), placed on the roads and parking lots for cars and for heavy goods vehicles, should endure a load of 400 kN. Since there is a lack of literature data of manhole cover optimization, this paper deals with analytical solution followed by numerical simulations.

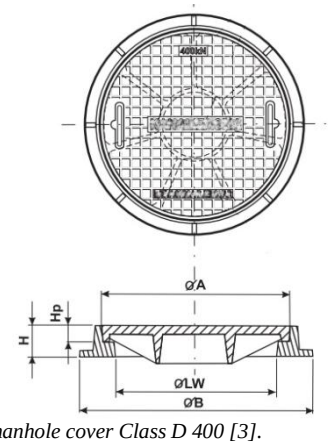

Fig. 1 *Circular manhole cover Class D 400 [3].*

2. Material and design

In this paper cover made of ductile iron (grade EN-GJS-500-7) with following dimensions was analyzed: diameter *A*=600 mm, height *H*p=50 mm, thickness 22 mm. The dimensions of the circular ribs are shown by the radial cross section on Fig. 2, while the position of the inner rib is variable at r = 80, 100, 120, 140, 160, 180, 200 mm.

According to EN 1563:2011 [4] mechanical properties of ductile iron grade EN-GJS-500-7 are following: modulus of elasticity E=169 GPa, Poisson's ratio ν =0.275, minimum tensile strength R_m=500 MPa, minimum 0.2% proof stress $R_{p0.2}$=320 MPa, minimum elongation A=7%. The microstructure of ductile iron grade EN-GJS-500-7 was observed by light microscope Olympus GX-51A. It consists of ferrite and pearlite (Fig.3).

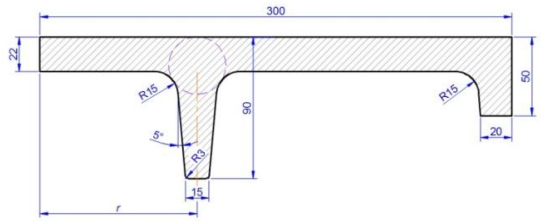

Fig. 2 *Dimensions of circular ribs (reinforcements) of manhole cover.*

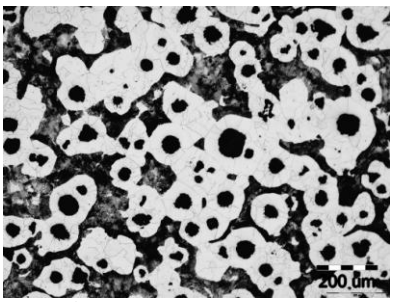

Fig. 3 *Microstructure of ductile iron grade EN-GJS-500-7.*

Firstly, the analytical analysis for bending of thin circular plate was conducted. Then, the same analysis was performed numerically using the software package Autodesk Simulation Mechanical [5] based on the finite element method. Results of the vertical displacement and radial and circular stresses, obtained by the numerical simulation, were compared with analytical solution. After the verification of numerical results of the bending of thin circular plate with analytical solution, the ribs on the bottom side of plate were gradually added. Optimal position of circular ribs and number of radial ribs will be calculated numerically using finite element method.

3. Analytical solution

Analytical solutions are only applicable for simple geometric problems such as bending of thin circular plate. A thin circular plate with a radius of R=300 mm by simply supported edge and loaded by uniformly continuous load q is presented in Fig. 4.

Internal transverse force Q was determined using the equilibrium condition for the radius r of the plate element according to Fig. 3b

$$\sum F_z = 2r\pi Q + r^2\pi q = 0\,. \quad (1)$$

The differential equation of bending the thin circular plate [6] is given by relation:

$$\frac{\mathrm{d}}{\mathrm{d}r}\left[\frac{1}{r}\frac{\mathrm{d}}{\mathrm{d}r}(\alpha\cdot r)\right] = \frac{Q}{D}\,, \quad (2)$$

where D is flexural stiffness of the thin plate expressed by

$$D = \frac{Eh^3}{12\left(1-\nu^2\right)}\,. \quad (3)$$

Rotation of the normal to the elastic line is represented by an angle α, which is variable in the radial direction [6] determined by the following expression:

$$\alpha = -\frac{\mathrm{d}w}{\mathrm{d}r}\,, \quad (4)$$

and represents the slope of the tangent to the elastic line (Fig. 4c).

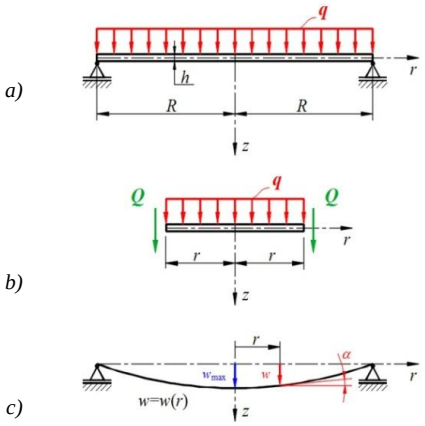

Fig. 4 *Bending of thin circular plate [6]: a) simply supported on the edge, b) internal transverse forces and c) elastic bending lines.*

Terms of normal stresses [6] in the radial (σ_r) and circular (σ_φ) direction are expressed with the following expressions:

$$\sigma_r = \frac{E}{1-\nu^2}\left(\frac{\mathrm{d}\alpha}{\mathrm{d}r} + \nu\frac{\alpha}{r}\right)z\,, \quad \sigma_\varphi = \frac{E}{1-\nu^2}\left(\frac{\alpha}{r} + \nu\frac{\mathrm{d}\alpha}{\mathrm{d}r}\right)z\,. \quad (5)$$

Inserting equations (1) and (3) into the equation (2), followed by its integration, and inserting two boundary conditions result in the expression for angle α: (i) complete plate (for r=0 → α=0) and (ii) there is no the bending moment on the outer edge (for r=R → M_r =0).

The necessary information about vertical displacement (deflection) w could be defined by rearranging equations (4) and by including the boundary condition of inability of deflection on the outer plate edge (for r=R → w=0). It is known that on the center of the plate the vertical displacement is maximal, as shown by the following expression

$$w_{\max} = \frac{5+\nu}{1+\nu}\cdot\frac{q\cdot R^4}{64\cdot D}\,. \quad (6)$$

Incorporating all known values for the material (E, ν), the load (q=F/($R^2\pi$)) and the geometry of the plate (D and h), the analytical solution of the maximal vertical displacement is achieved. Maximal vertical displacement for ductile iron grade EN-GJS-500-7 is 4.59 mm.

The design process has to ensure that the maximum calculated (equivalent) stress (σ_{equ}) is less than the allowable stress ($\sigma_{\mathrm{equ}} \le \sigma_{\mathrm{allow}}$). For ductile materials, such as nodular cast iron, the allowed stress (σ_{allow}) is calculated according to the expression

$$\sigma_{\mathrm{allow}} = \frac{R_{\mathrm{p0.2}}}{fs}\,, \quad (7)$$

where f_s is the safety factor. In this paper taken safety factor is f_s=2. Allowed stress for ductile iron grade EN-GJS-500-7 are 160 MPa.

4. Numerical solution

The analysis of the circular manhole covers was being conducted by software package Autodesk Simulation Mechanical [5] based on the finite element method. The purpose of this paper was to analyse the influence of ribs on strength of circular manhole cover in three variants of circular plates:

(I) thin circular plate without ribs (Fig. 5a),

(II) thin circular plate with two circular ribs added on the bottom side: lower on the outer circumference and higher on the inner circumference the radius that will change (Fig. 5b). Position of the internal rib is variable at r = 80, 100, 120, 140, 160, 180 and 200 mm.

(III) thin circular plate with several (6,7 and 8) radial ribs connected with the circular ribs on the bottom side (Fig. 5c).

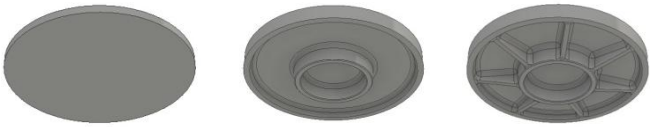

Fig. 5 *Circular manhole cover: a) Variant I, b) Variant II, c) Variant III.*

In numerical analysis it is not necessary to model the entire manhole covers in all three variants. Variants I and II of the covers are axially symmetric and the analysis can be conducted by the axisymmetric elements. Because of radial ribs, the Variant III of the manhole cover is not completely axisymmetric. Therefore, all numerical analyses will be conducted in such a way that the cover on the upper surface is divided into equal parts in the circular direction. The plate geometry of Variants I and II was observed at an angle of 60 °, while in Variant III depending on the number of added radial ribs angle varied as follows: 360°/6, 360°/7 and 360°/8.

All geometries of circular covers was being modeled by the software package Autodesk Inventor Professional [7], and imported to the software package Autodesk Simulation Mechanical [5] to be performed the preprocessing. Imported geometric domain is divided into a network of finite elements on which are associated material properties, natural boundary conditions (q) and geometric boundary conditions shown in Fig. 6. Before defining the boundary conditions, it is necessary to set up a cylindrical coordinate system.

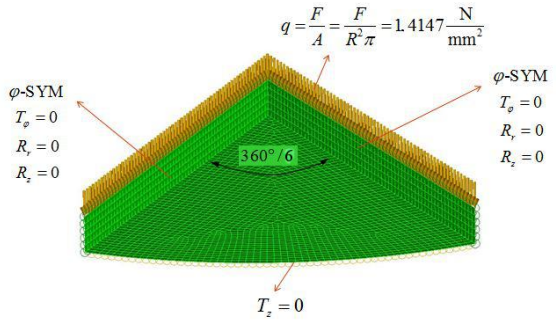

Fig. 6 *Natural and geometric boundary condition applied on thin circular plate (Variant I).*

Load of F=400 kN in the form of pressure q (q=F/($R^2\pi$)) over the entire upper surface of circular manhole cover is added (Figure 5) and the following boundary conditions are defined as follows: (i) at the outer bottom periphery edge the condition of prevented displacement in z direction (T_z=0) and (ii) based on a cylindrical coordinate system at the radial sections the boundary conditions of φ-symmetry (T_φ=0, R_r=0 and R_z=0).

In the numerical simulations the equivalent stresses based on the energy theory of strength (von Mises) were monitored. After preprocessing, the three-dimensional linear static analyses of all three variants of cover are performed. The results of these analyses are presented in the next section.

5. Results and discussion

Results of numerical analysis of bended thin circular plate (Variant I) displacement in the *z* direction (deflection) and equivalent stress are shown in Figure 7a and 7b, respectively.

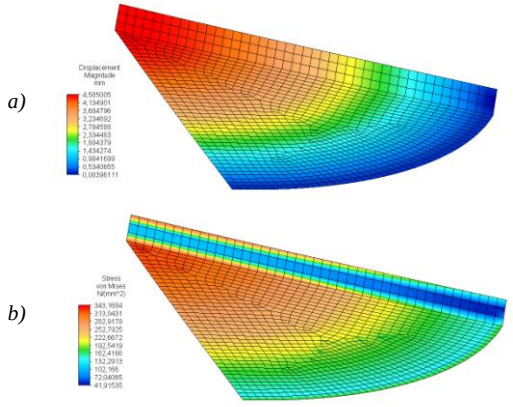

Fig. 7 Results of vertical displacement (a) and equivalent stress (b) for bending of thin circular plate (Variant I).

It is obvious that deflection and equivalent stress are greatest in the center of the plate. Results of radial and circular stresses are presented in Figure 8a and 8b, respectively.

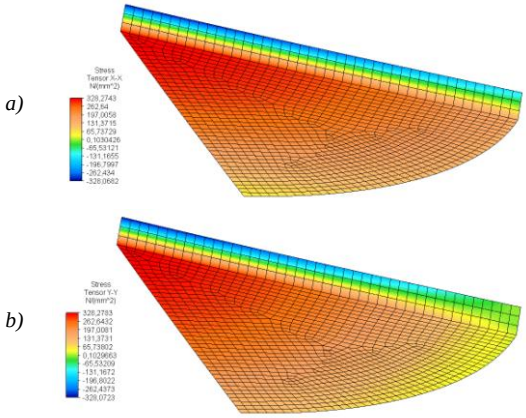

Fig. 8 Results of radial (a) and circular (b) stresses for bending of thin circular plate (Variant I).

Analytical and numerical solutions for maximal deflection and maximal radial and circular stresses are compared in Table 1. It can be seen a very good agreement of numerical results with analytical which implies a verification of numerical analysis by analytical solution.

Table 1: *Comparison of analytical and numerical solutions for bending the thin circular plates (Variant I).*

	Analytical solution	Numerical solution
w_{max}, mm	4.57	4.59
σ_r, N/mm^2	±323.08	+328.27 -328.07
σ_φ, N/mm^2	±323.08	+328.27 -328.07

The maximal equivalent stress, obtained numerically using the energy theory of strength (von Mises), is 343.17 N/mm^2 (Fig. 7b). It could be seen that in case of the analysis of Variant I (Fig. 5a) the condition of strength is not achieved.

For this reason, two circular vertical ribs are added on the bottom side of existing thin circular plate (Fig. 4b, Variant II): internal and external. The dimensions of the circular ribs are shown on the radial cross section of Fig. 2, while the position of the internal rib is variable at r = 80, 100, 120, 140, 160, 180 and 200 mm.

Results of several numerical analysis of bending of circular manhole cover with two circular ribs (Variant II) of maximal displacement (deflection) in the *z* direction are shown in Fig. 9a. On Fig. 9b for position of internal circular ribs of r=120 mm vertical displacement magnitude are presented.

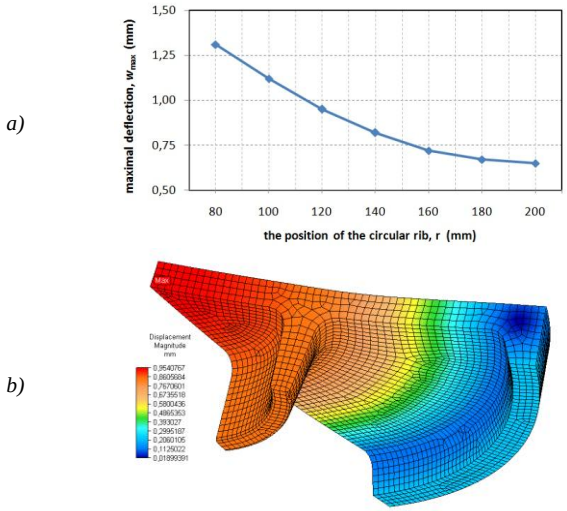

Fig. 9 (a) Dependence of the maximal vertical displacement on the position of the inner circular rib and (b) numerical results of vertical displacement for bending circular manhole cover with two circular ribs (r=120 mm) (Variant II).

The analysis of results of maximal deflection at center of cover shows that by increasing the radius of the internal circular rib (Fig. 9a) maximal vertical displacement decrease.

Results of several numerical analysis of bending of circular manhole cover with two circular ribs (Variant II) of equivalent stress are shown in Fig. 10a. On Fig. 10b for position of internal circular ribs of r=120 mm equivalent stress are present.

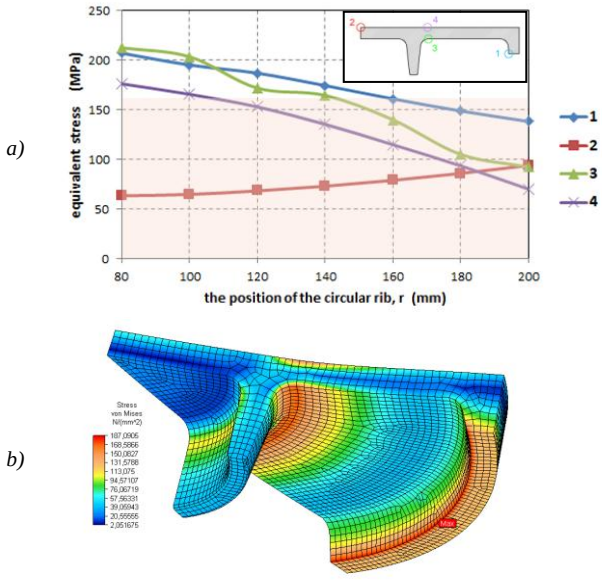

Fig. 10 (a) Dependence of the maximal vertical displacement on the position of the inner circular rib and (b) numerical results of vertical displacement for bending circular manhole cover with two circular ribs (r=120 mm) (Variant II).

The analysis of results of equivalent stresses shows that by increasing the radius of the internal circular rib (Fig. 10a), stresses decrease in the positions 1, 3 and 4, while at the center of cover (position 2) increase. In the diagram (Fig. 10a) the area of allowable stress is indicated by another color (beige). For further analysis, based on the Fig.1 the position of the internal rib at r = 120 mm is chosen. The stresses which are greater than those allowed in positions 1 and 3 will be reduced by addition of radial ribs.

On the model of Variant II with r = 120 mm radial ribs located from the inner to outer circular ribs, is added. The radial ribs are 15 mm thick. Numerical simulation of bending of circular manhole

cover with 6, 7 and 8 radial ribs is performed. The results of the numerical analysis of the vertical displacement and the equivalent stresses with seven radial ribs are shown at Fig. 11 and Fig. 12, respectively.

a)

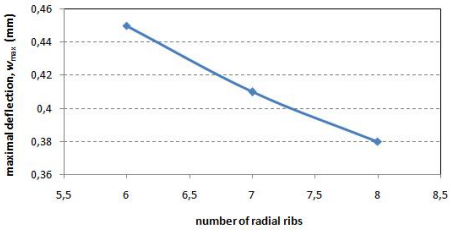

b)

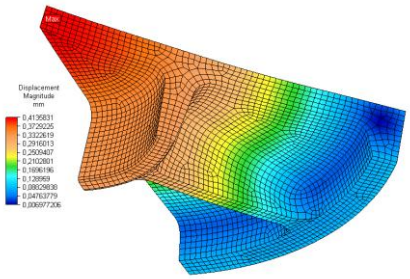

Fig. 11 *(a) Dependence of the maximal vertical displacement on the number of radial ribs and (b) numerical results of vertical displacement for bending circular manhole cover with two circular ribs (r=120 mm) and seven radial ribs (Variant III).*

The analysis of results of maximal deflection at the center of cover shows that by increasing the number of radial ribs (Fig. 11a) maximal vertical displacement decreases.

a)

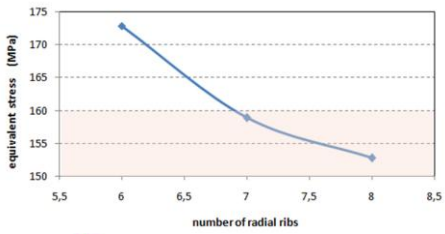

b)

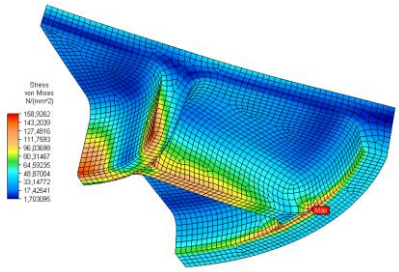

Fig. 12 *(a) Dependence of the maximal equivalent stress on the number of radial ribs and (b) numerical results of equivalent stress for bending circular manhole cover with two circular ribs (r=120 mm) and seven radial ribs (Variant III).*

The analysis of results of equivalent stresses show that by increasing number of radial ribs (Fig. 12a) maximal stresses decrease. In the diagram presented in Fig. 12a the area of allowable stress is indicated by another color (beige). Design of circular manhole cover of Variant III with more than six radial ribs is allowed, because equivalent stresses are less than the allowable stress ($\sigma_{equ} \leq \sigma_{allow}$). Design of circular manhole cover with seven radial ribs is optimal.

Schematic representation of all numerical results of maximal equivalent stresses on Variant I, II and III in stress-strain diagram of used ductile iron on Fig. 13 is presented.

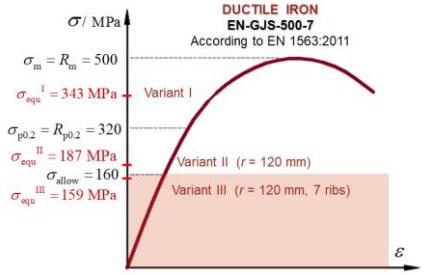

Fig. 13 *Schematic representation of numerical results of maximal equivalent stress in stress-strain diagram of ductile iron.*

By adding the circular and radial ribs on the bottom side of the thin circular plate, the maximum deflection at the centre of the cover decreases ($w_{max,I} > w_{max,II} > w_{max,III}$).

6. Conclusions

The purpose of this paper was to analyse the influence of ribs on strength of circular manhole cover in three variants of thin circular plate:

(I) thin circular plate without ribs (Fig. 5a) – Variant I,

(II) thin circular plate with two circular ribs added on the bottom side: lower on the outer circumference and higher on the inner circumference the radius that will change (Fig. 5b). Position of the internal rib is variable at *r* = 80, 100, 120, 140, 160, 180 and 200 mm – Variant II.

(III) thin circular plate with several (6,7 and 8) radial ribs connected with the circular ribs on the bottom side (Fig. 5c) – Variant III.

Numerical solution for bending thin circular plate (Variant I) is compared with analytical solution. For Variant II and III of manhole cover numerical simulation of bending are conducted.

It is important to note that the equivalent stresses in the plate of Variant I exist in the center of the plate, in Variant II are moved closer to the internal circular rib and in Variant III lower to the top of the circular rib. Results of numerical simulations showed that increase in number of radial ribs decrease the maximal vertical displacement and equivalent stress. Finally, it can be concluded that optimal design of circular manhole cover is made of seven radial ribs connected with the circular ribs on the bottom side of cover.

7. References

[1] El Haggar S., El Hotow L., Reinforcement of thermoplastic reject in the production of manhole covers, Journal of Cleaner Production, 17(2009), 440-446.

[2] Draman, W.N.A.W., Majid, D.L., Ishak, M.I., Rosli, M.U., Lailina, N.M., Ismail, R.I., An auto lifting device to lift manhole cover with ergonomics consideration, (2017) AIP Conference Proceedings 1885, 020067, doi: 10.1063/1.5002261

[3] Kanalska galanterija (HRN EN-124:2005), Accessible on Internet: http://www.aqua-invest.hr/images/stories/down/kanalska_galanterija.pdf, 2.11.2017.

[4] … EN 1563:2011, Founding - Spheroidal graphite cast irons, European committee for standardization, 2011.

[5] Autodesk Simulation Mechanical: Tutorial, Accessible on Internet: https://knowledge.autodesk.com/support/simulation-mechanical, 2.11.2017.

[6] Alfirević I., Nauka o čvrstoći II, Golden marketing, Zagreb, 1999.

[7] Autodesk Inventor Professional: Tools and Design, Accessible on Internet: http://www.sdcpublications.com/pdfsample/978-1-58503-958-6-7.pdf, 2.11.2017.